Available on CMS information server

CMS CR -2012/175

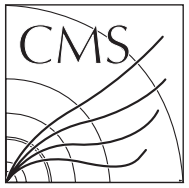

The Compact Muon Solenoid Experiment

Conference Report

Mailing address: CMS CERN, CH-1211 GENEVA 23, Switzerland

26 July 2012 (v3, 31 July 2012)

Azimuthal anisotropy in charged hadron production in 2.76 TeV PbPb collisions measured by CMS

Eric Andrew Appelt for the CMS Collaboration

Abstract

We report on the CMS measurements of charged hadron anisotropic azimuthal distributions from PbPb collisions at a center-of-mass energy of 2.76 TeV per nucleon pair and their decomposition into a Fourier series up to the 6th coefficient. The results are presented as a function of transverse momentum, centrality and pseudorapidity and cover a broad kinematic range. These results can provide constraints on the theoretical description of the early dynamics in the hot and dense medium and its transport properties.

Presented at *WWND12: 28th Winter Workshop on Nuclear Dynamics*

Azimuthal Anisotropy in Charged Hadron Production in 2.76 TeV PbPb Collisions Measured by CMS

Eric Appelt on behalf of the CMS Collaboration
Vanderbilt University, Nashville, United States
E-mail: eric.appelt@gmail.com

Abstract. We report on the CMS measurements of charged hadron anisotropic azimuthal distributions from PbPb collisions at a center-of-mass energy of 2.76 TeV per nucleon pair and their decomposition into a Fourier series up to the 6th coefficient. The results are presented as a function of transverse momentum, centrality and pseudorapidity and cover a broad kinematic range. These results can provide constraints on the theoretical description of the early dynamics in the hot and dense medium and its transport properties.

1. Introduction

The azimuthal anisotropy of charged hadrons produced in PbPb collisions are typically characterized by the coefficients (v_n) of Fourier harmonics in an azimuthal distribution (ϕ) of the charged particle yield, $dN/d\phi \propto 1 + \sum_{n=1}^{\infty} 2v_n \cos\left(n(\phi - \Psi_R)\right)$, where Ψ_R is a reference angle determined event-by-event that corresponds to a "participant plane". The coefficient v_2, commonly referred to as the elliptic flow coefficient, is dominant in non-central events due to the typically lenticular shape of the overlap region of the colliding nuclei. Particularly for the measurement of v_2, the participant plane is defined by the minor axis of the overlap region and the beam direction. The results presented here include detailed measurements of the elliptic flow of charged particles produced in PbPb collisions at $\sqrt{s_{NN}} = 2.76$ TeV in a broad kinematic range of $|\eta| < 2.4$, and $0.3 < p_T < 60$, in the centrality range of 0-80% of the total inelastic PbPb cross-section. Additionally, preliminary results for higher flow harmonic coefficients ranging from v_3 to v_6 are presented.

In the low-p_T region, these coefficients are generally associated with the hydrodynamic flow of the medium produced in the collision [1]. Event-by-event fluctuations in the value of v_2 may be driven by fluctuations in the shape of the initial overlap area [2], and different experimental methods for measuring v_2 can respond differently to these fluctuations [3]. In addition, measurements of v_2 at low-p_T may be affected by "non-flow" particle correlations from jets and resonance decays. Multiple methods are therefore employed to measure the flow harmonics in order to better understand the initial state of the collision and the hydrodynamic properties of the medium.

At high-p_T, a non-zero value of v_2 can be induced if there is a stronger suppression of the hadron yield along the long axis than the short axis of the overlap region. The measurement of v_2 at high-p_T can quantitatively constrain models of partonic energy loss in the medium that

take account of the influence of the path length and shape of the overlap region of the colliding nuclei.

2. Experimental method

These measurements were taken with the Compact Muon Solenoid (CMS) detector using $\sqrt{s_{NN}} = 2.76$ TeV data obtained during the 2010 and 2011 heavy-ion runs at the Large Hadron Collider (LHC). The CMS detector primarily consists of a silicon tracker, lead-tungstenate electromagnetic calorimeter, brass/scintillator hadronic calorimeter, and gas-ionization muon chambers. The tracker and calorimeters are housed within a 3 m radius superconducting solenoid that provides a 3.8T magnetic field. In addition, the detector includes extensive forward calorimetry including two steel/quartz Čerenkov Hadron Forward (HF) calorimeters, and Beam Scintillation Counters (BSC) placed along the beamline. The silicon tracker is comprised of a inner silicon pixel detector and outer silicon strip detector. A more detailed description of the CMS detector can be found elsewhere [4].

2.1. Event selection and tracking

Minimum bias PbPb events were triggered via coincident signals from both ends of the detector in either the BSC or HF calorimeters. Additional offline event selection was performed in order to remove events due to noise, beam backgrounds, electromagnetic interactions leading to the breakup of nuclei, and other non-collision events [5]. The minimum bias trigger has an acceptance of $(97 \pm 3)\%$ for inelastic hadronic PbPb collisions. For the 2011 heavy-ion run, only a small fraction of all minimum-bias triggered events could be recorded due to hardware limits on the data acquisition rate. In order to maximize the sample of events containing high-p_T particles emitted in PbPb collisions, a dedicated high-p_T single track trigger was implemented, utilizing a tracking algorithm identical to the offline track reconstruction which identified high-p_T charged particles starting with a candidate trajectory from the three-layer silicon pixel detector with $p_T > 11$ GeV/c. [6] The efficiency of this high-p_T track trigger rises from about 75% at $p_T \approx 12$ GeV/c to nearly 100% above $p_T \approx 20$ GeV/c.

The algorithm used to reconstruct charged particle tracks for the 2010 analyses presented here employed a two-iteration tracking algorithm, with one iteration using only the pixel detector to reconstruct charged particles with a p_T as low as 0.3 GeV/c, and is described in detail in Ref. [5]. The charged particle reconstruction algorithm used for the 2011 data used multiple iterations to provide good efficiency at very high-p_T, and is described in detail in Ref. [7].

2.2. Centrality and Glauber modeling

Centrality determination was performed using the total energy in both of the HF detectors. Using this total energy distribution, the event samples were divided into 40 centrality bins, each representing 2.5% of the total inelastic nucleus-nucleus cross section. These small bins are then regrouped into centrality classes ranging from 0% to 80% for the various analyses.

The Monte Carlo Glauber model is a multiple collision model that treats each nucleus-nucleus collision as an independent sequence of nucleon-nucleon collisions. From this model, quantities of interest characterizing the events of each centrality class that are not directly observable are calculated, such as the number of participating nucleons, or N_{part}. The eccentricity of the overlap region of the colliding nuclei as determined by this model, called the participant eccentricity, is denoted here as ϵ_{part} or just ϵ. Additionally, the cumulant moments, defined as $\epsilon\{2\}^2 \equiv \langle\epsilon^2_{\mathrm{part}}\rangle$ and $\epsilon\{4\}^4 \equiv 2\langle\epsilon^2_{\mathrm{part}}\rangle^2 - \langle\epsilon^4_{\mathrm{part}}\rangle$, are calculated from this model.

2.3. Methods for measuring the anisotropy parameters

The value of v_n measured by the event-plane method, denoted here as $v_n\{\mathrm{EP}\}$, is defined as $v_n\{\mathrm{EP}\} = \langle\cos n(\phi - \psi_{\mathrm{EP}})\rangle/R$. Here ψ_{EP} denotes a reconstructed event-plane, in this analysis

determined from the azimuthal energy distribution in the HF calorimeters. R represents a correction factor for the resolution of the reconstructed event-plane, and the average is taken over all particles in all events [8].

The cumulant methods measure flow by a cumulant expansion of the multiparticle azimuthal correlations, without determining the orientation of the event-plane. The value of v_n measured by the two-particle cumulant method, denoted here as $v_n\{2\}$, is defined as $v_n\{2\} = \sqrt{\langle \cos n(\phi_1 - \phi_2)\rangle}$ where ϕ_1 and ϕ_2 represent the azimuthal angles of two charged particles and the average is taken over all pairs of particles in all events. The two-particle cumulant method is particularly sensitive to non-flow. The value of v_n measured by the four-particle cumulant method, denoted here as $v_n\{4\}$, is similarly defined as $v_n\{4\} = (2\langle \cos n(\phi_1 - \phi_2)\rangle^2 - \langle \cos n(\phi_1 + \phi_2 - \phi_3 - \phi_4)\rangle)^{1/4}$. The four-particle cumulant method removes lower order non-flow effects from correlations between pairs of particles. For both the two- and four-particle cumulant methods, $v_n\{2\}$ and $v_n\{4\}$ are estimated using a generating function of the multiparticle correlations in the complex plane [9].

The Lee–Yang zeros method, from which the measured value of v_2 is denoted here as $v_2\{\mathrm{LYZ}\}$, is based on multiparticle correlations involving all particles in the event. Using the asymptotic behavior of the cumulant expansion, the location of the zeros of a complex function are related to the magnitude of the integrated flow in the system [10]. The Lee–Yang zeros method approximates a cumulant of very high order and removes the influence of non-flow from the measured v_2 signal.

A much more detailed description of the methods used in these analyses is given in Ref. [5] and the references contained therein.

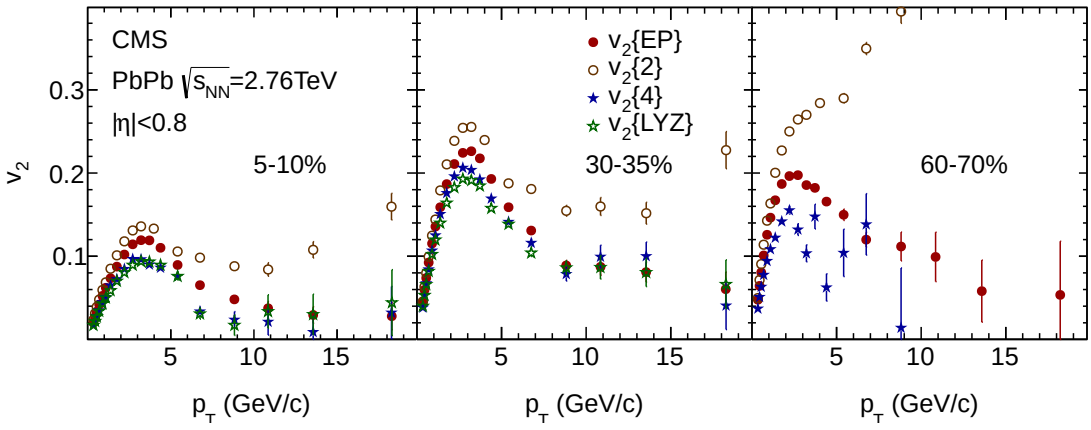

Figure 1. Comparison of the four different methods for measuring v_2 as a function of p_T at mid-rapidity ($|\eta| < 0.8$) for three representative centrality classes given in the figures [5]. The error bars show the statistical uncertainties only.

3. Elliptic flow at midrapidity

In Fig. 1, the v_2 measurement as a function of p_T is given at midrapidity ($|\eta| < 0.8$) for the event-plane, two-particle cumulant, four-particle cumulant, and Lee–Yang zeros methods, denoted as $v_2\{\mathrm{EP}\}$, $v_2\{2\}$, $v_2\{4\}$, and $v_2\{\mathrm{LYZ}\}$, respectively. Excepting the $v_2\{2\}$ results in

peripheral events which are dominated by non-flow effects at high-p_T, the transverse momentum dependence shows a rise of v_2 up to $p_T \approx 3$ GeV/c and then a decrease.

In the left panel of Fig. 2, the v_2 obtained from the event-plane and cumulant methods at midrapidity is integrated over the range $0.3 < p_T < 3.0$, scaled by the participant eccentricity as determined from the Glauber-model simulation, and plotted as a function of centrality. These data show a near-linear decrease in the eccentricity scaled v_2 from central to peripheral collisions. The values of v_2 from the cumulant methods were scaled with their respective cumulant moments of the participant eccentricity, which following the definition of $v_2\{2\}$ and $v_2\{4\}$ may be written [3]:

$$\frac{v_2\{2\}}{\epsilon\{2\}} = \left(\frac{\langle v_2^2\rangle}{\langle \epsilon^2\rangle}\right)^{1/2}, \quad \text{and} \quad \frac{v_2\{4\}}{\epsilon\{4\}} = \left(\frac{2\langle v_2^2\rangle^2 - \langle v_2^4\rangle}{2\langle \epsilon^2\rangle^2 - \langle \epsilon^4\rangle}\right)^{1/4}, \tag{1}$$

where $\langle v_2\rangle$ represents the event-by-event average of the v_2 value from each event. If the hydrodynamic response to the participant eccentricity is linear, i.e. $v_2 \sim \epsilon$, and nonflow effects are negligible, then the identity $v_2\{2\}/\epsilon\{2\} = v_2\{4\}/\epsilon\{4\}$ should hold [2]. In the right panel of Fig. 2, $v_2\{2\}/\epsilon\{2\}$ and $v_2\{4\}/\epsilon\{4\}$ are plotted and agree in the centrality range of 15-40%, suggesting that the difference between these methods can be attributed to their respective sensitivities to event-by-event flow fluctuations.

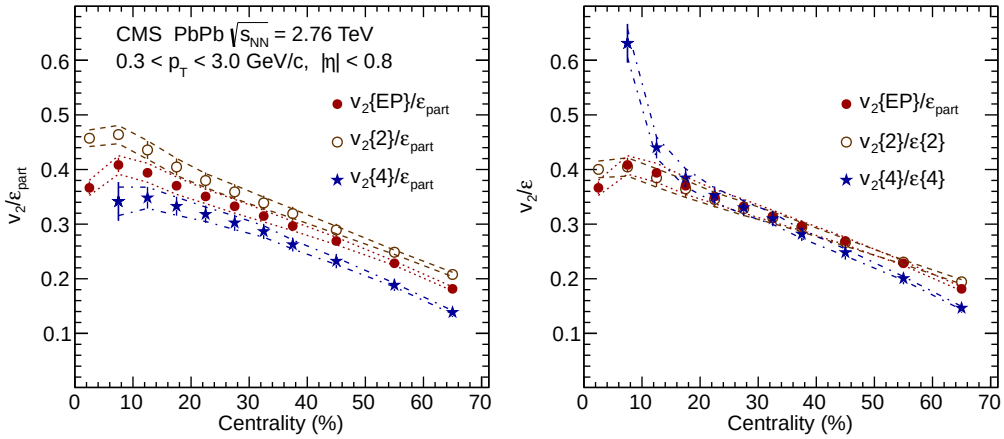

Figure 2. Left panel: Centrality dependence of the p_T-integrated v_2 divided by the participant eccentricity, $\varepsilon_{\rm part}$, measured at mid-rapidity ($|\eta| < 0.8$) for the event-plane, two-particle cumulant, and four-particle cumulant methods [5]. Right panel: The same measurements as in the left panel, but here the two-particle and four-particle cumulant results are divided by their corresponding moments of the participant eccentricity, $\varepsilon\{2\}$ and $\varepsilon\{4\}$. In both panels the error bars show the sum in quadrature of the statistical and systematic uncertainties in the measurement of v_2, and the lines show the systematic uncertainties in the eccentricity determination.

4. Elliptic flow at forward rapidity

The measurement of $v_2(\eta)$ integrated over the range $0.3 < p_T < 3.0$ for the four methods is shown in three representative centrality classes in Fig. 3. The values for $v_2\{4\}$ and $v_2\{\text{LYZ}\}$ are in agreement and smaller than $v_2\{\text{EP}\}$ and $v_2\{2\}$. The value of $v_2(\eta)$ is greatest at midrapidity and slowly decreases at higher values of $|\eta|$. This decrease is more pronounced in the more peripheral collisions.

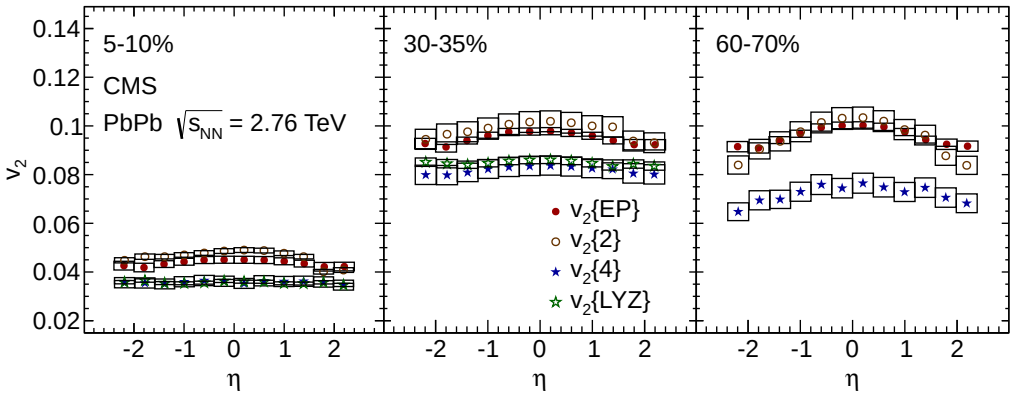

Figure 3. Pseudorapidity dependence of v_2 integrated over the range $0.3 < p_T < 3$ GeV/c for all four methods in three representative centrality classes [5]. The error bars show the statistical uncertainties, and the boxes show the systematic ones.

To ascertain whether the decrease in $v_2(\eta)$ at high $|\eta|$ is due to a change in the underlying spectra, or if it is due to a pseudorapidity dependence of $v_2(p_T)$, a measurement of $v_2(p_T)$ with the event-plane method in three pseudorapidity intervals is displayed in Fig. 4. For the events from 0-40% centrality, the $v_2(p_T)$ distribution is not seen to change with pseudorapidity within statistical uncertainties, indicating that any change in $v_2(\eta)$ is due to the underlying charged particle spectra. For more peripheral events, a slight decrease in $v_2(p_T)$ is observed at high $|\eta|$, indicating that a pseudorapidity dependence of the $v_2(p_T)$ distribution contributes to the decrease in $v_2(\eta)$ with increasing $|\eta|$ in peripheral events.

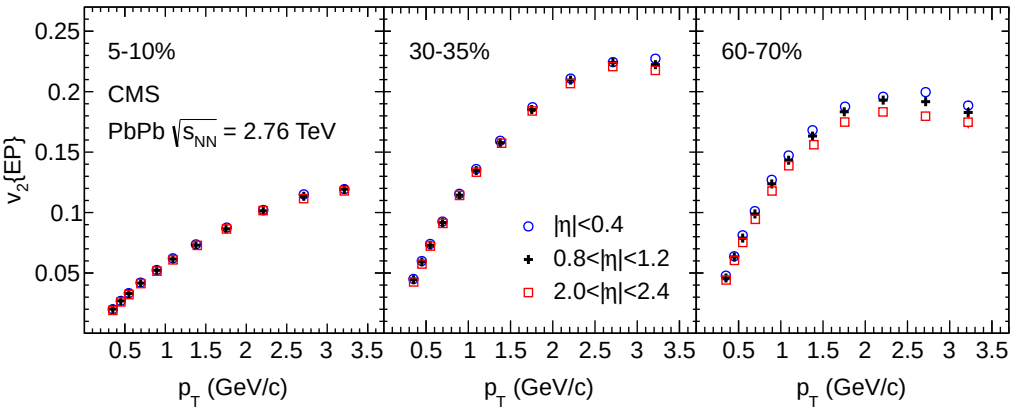

Figure 4. $v_2(p_T)$ as measured by the event-plane method in three pseudorapidity regions and in three representative centrality classes [5]. The error bars show the statistical uncertainties.

The PHOBOS experiment at the Relativistic Heavy Ion Collider (RHIC) has observed that the v_2 over a large range of collision energies ranging from $\sqrt{s_{NN}} = 19.6$ GeV to 200 GeV exhibited extended longitudinal scaling when viewed from the rest frame of one of the colliding nuclei [11]. As the measured particles are unidentified in both the CMS and PHOBOS

measurements, the pseudorapidity η^+ (η^-) of the particles in the rest frame of the nucleus moving in the positive (negative) direction is given by $\eta^{\pm} = \eta \pm y_{\rm beam}$ where η is the pseudorapidity of the particles in the laboratory or center-of-mass frame, and $y_{\rm beam} \approx \ln \sqrt{s_{NN}}$[GeV]. In Fig. 5, the left (right) half of each plot shows v_2 in the rest frame of the beam moving in the positive (negative) direction. The CMS results plotted here are obtained from the event-plane method integrated over the range $0 < p_T < 3.0$, where values of $v_2(p_T)$ below $p_T = 0.3$ GeV/c are estimated by extrapolating the charged particle spectrum and $v_2(p_T)$ distribution to $p_T = 0$ by assuming that $v_2(p_T = 0) = 0$. Although the CMS data cover 4.8 units of pseudorapidity, they do not overlap the PHOBOS data when plotted in the rest frames of the colliding nuclei due to the extreme difference in beam energies. The CMS data show a weaker pseudorapidity dependence than the PHOBOS data, and suggest a nearly boost-invariant region which is wider in η for more central events.

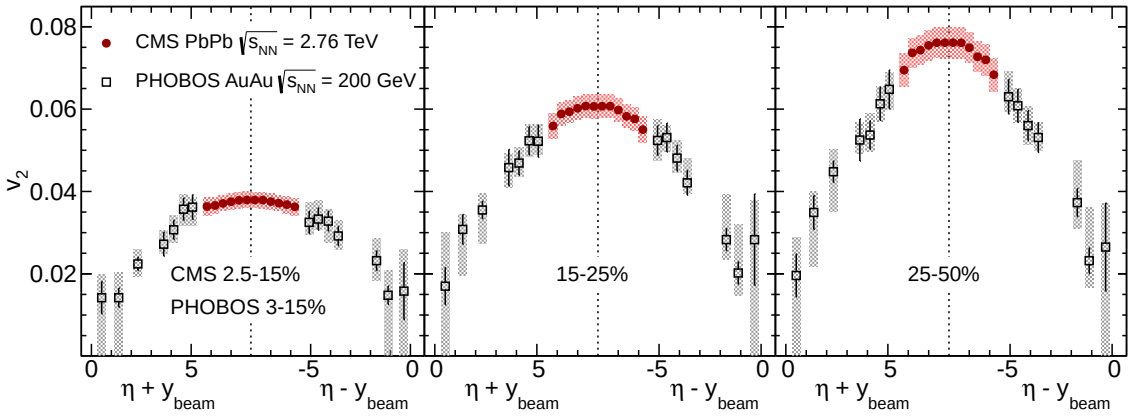

Figure 5. Measured $v_2(\eta)$ from CMS [5] (closed symbols) and PHOBOS [12] (open symbols) in three centrality intervals. The left (right) half of each plot shows v_2 in the rest frame of the beam moving in the positive (negative) direction. The error bars show the statistical uncertainties, and the boxes show the systematic ones.

5. Higher order flow

Preliminary measurements of higher order flow harmonics from v_3 to v_6 have been taken from the 2010 heavy-ion data using the two-particle cumulant, three-particle cumulant, five-particle cumulant, and Lee–Yang zeros methods [13]. In Fig. 6, measurements the $v_2\{4\}$, $v_3\{2\}$, $v_4\{3\}$, $v_4\{5\}$, $v_4\{\text{LYZ}\}$, and $v_6\{\text{LYZ}\}$ methods have been integrated over the range $0.3 < p_T < 3.0$ and are given a function of the number of participant nucleons corresponding to each centrality bin as estimated by MC Glauber simulations. [13] The value of v_3 increases slowly from central to peripheral collisions, reaches a maximum at around $N_{\rm part} = 100$, then decreases slightly. This is in contrast to v_2, which increases rapidly with centrality and saturates at approximately the same value of $N_{\rm part}$ as the measured v_3.

6. Azimuthal anisotropy at extremely high transverse momentum

The results for $v_2(p_T)$ for p_T ranging from 1 GeV/c to 60 GeV/c taken from the 2011 heavy-ion data using the event plane method in six centrality ranges from 0-10% to 50-60% are shown in Fig. 7. These new CMS results significantly extend the p_T reach of previous v_2 measurements achieved by the ALICE [14], ATLAS [15], and CMS [5] Collaborations. Beyond $p_T = 10$ GeV/c

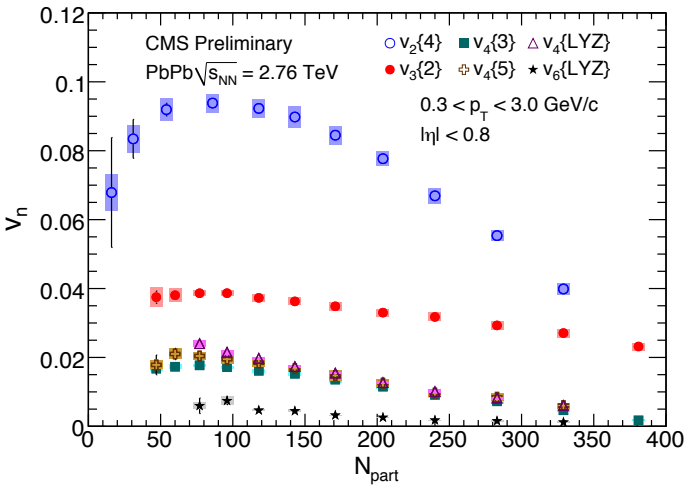

Figure 6. Integrated $v_2\{4\}$, $v_3\{2\}$, $v_4\{3\}$, $v_4\{5\}$, $v_4\{\mathrm{LYZ}\}$, and $v_6\{\mathrm{LYZ}\}$ as a function of the number of participant nucleons corresponding to each centrality bin as estimated by MC Glauber simulations. [13]. The error bars show the statistical uncertainties and the colored bands show the systematic ones

the value of v_2 shows a much weaker dependence on p_T than at lower transverse momenta, and the values of v_2 continue to gradually decrease but remain greater than zero up to $p_T = 40$ GeV/c.

This result indicates a clear dependence of v_2 on p_T in this extremely high-p_T region where the charged particle production is dominated by parton fragmentation and energy-loss models are most applicable. This suggests that the path-length dependence of partonic energy loss in the medium is itself dependent on the initial energy of the parton.

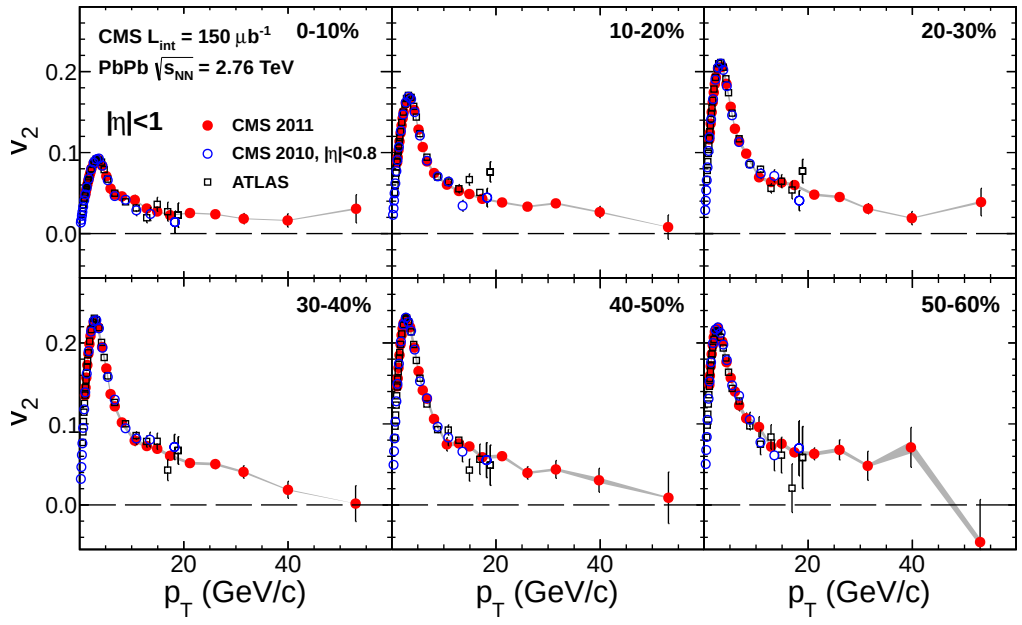

Figure 7. $v_2(p_T)$ from 1.0 to 60.0 GeV/c with $|\eta| < 1$ for six centrality ranges in PbPb collisions at $\sqrt{s_{NN}} = 2.76$ TeV, Solid markers indicate the results from CMS using data collected in 2011 [6]. For comparison, results from the ATLAS [15] experiment are shown in open squares, and earlier CMS results from data collected in 2010 are shown in open circles [5]. Error bars show the statistical uncertainties, while the grey bands correspond to the systematic uncertainties.

7. Summary

Detailed measurements of the azimuthal anisotropies for charged particles in $\sqrt{s_{NN}} = 2.76$ TeV PbPb collisions have been presented. Four methods have been used to determine the value of v_2 as a function of transverse momentum, pseudorapidity, and centrality in the broad kinematic range of $0.3 < p_T < 20$ and $|\eta| < 2.4$. The value of $v_2(p_T)$ has been found to increase up to $p_T \approx 3$ GeV/c and then slowly decrease. The measurement of $v_2(p_T)$ with the event-plane method was greatly expanded to $p_T = 60$ GeV/c using the enhanced statistics of the 2011 heavy-ion data produced by the single-track trigger. A non-zero value of v_2 was observed at a value of at least $p_T = 40$ GeV/c. The value of $v_2(\eta)$ was found to have a weak dependence on pseudorapidity in central collisions, and as $|\eta|$ increases the value of $v_2(\eta)$ gradually drops in peripheral collisions. Comparisons of $v_2(\eta)$ to PHOBOS data suggested that extended longitudinal scaling may hold to LHC energies. Preliminary measurements of higher order flow harmonics ranging from v_3 to v_6 have also been presented. The precision data over a wide kinematic range presented here will provide important constraints on the initial state of the collision, the hydrodynamic properties of the medium formed in the collision, and models of partonic energy loss in the medium.

Acknowledgments

We congratulate our colleagues in the CERN accelerator departments for the excellent performance of the LHC machine. We thank the technical and administrative staff at CERN and other CMS institutes, and acknowledge support from: BMWF and FWF (Austria); FNRS and FWO (Belgium); CNPq, CAPES, FAPERJ, and FAPESP (Brazil); MES (Bulgaria); CERN; CAS, MoST, and NSFC (China); COLCIENCIAS (Colombia); MSES (Croatia); RPF (Cyprus); MoER, SF0690030s09 and ERDF (Estonia); Academy of Finland, MEC, and HIP (Finland); CEA and CNRS/IN2P3 (France); BMBF, DFG, and HGF (Germany); GSRT (Greece); OTKA and NKTH (Hungary); DAE and DST (India); IPM (Iran); SFI (Ireland); INFN (Italy); NRF and WCU (Korea); LAS (Lithuania); CINVESTAV, CONACYT, SEP, and UASLP-FAI (Mexico); MSI (New Zealand); PAEC (Pakistan); MSHE and NSC (Poland); FCT (Portugal); JINR (Armenia, Belarus, Georgia, Ukraine, Uzbekistan); MON, RosAtom, RAS and RFBR (Russia); MSTD (Serbia); SEIDI and CPAN (Spain); Swiss Funding Agencies (Switzerland); NSC (Taipei); TUBITAK and TAEK (Turkey); STFC (United Kingdom); DOE and NSF (USA).

This research is supported in part by the Department of Energy Office of Science Graduate Fellowship Program (DOE SCGF), made possible in part by the American Recovery and Reinvestment Act of 2009, administered by ORISE-ORAU under contract no. DE-AC05-06OR23100.

References

[1] Voloshin S, Poskanzer A and Snellings R 2008 (*Preprint* `nucl-ex/0809.2949`)
[2] Qiu Z and Heinz U 2011 *Phys. Rev. C* **84** 024911
[3] Ollitrault J Y, Poskanzer A and Voloshin S 2009 *Phys. Rev. C* **80** 014904
[4] CMS Collaboration 2008 *JINST* **3** S08004
[5] CMS Collaboration 2012 Submitted for publication in *Phys. Rev. C* (*Preprint* `nucl-ex/1204.1409`)
[6] CMS Collaboration 2012 *Phys. Rev. Lett.* **109** 022301
[7] CMS Collaboration 2012 *Eur. Phys. J. C.* **72** 1945
[8] Poskanzer A and Voloshin S 1998 *Phys. Rev. C* **58** 1671
[9] Borghini N, Dinh P and Ollitrault J Y 2001 *Phys. Rev. C* **64** 054901
[10] Bhalerao R, Borghini N and Ollitrault J Y 2003 *Nucl. Phys. A* **727** 373
[11] PHOBOS Collaboration 2005 *Phys. Rev. Lett.* **94** 122303
[12] PHOBOS Collaboration 2005 *Phys. Rev. C* **72** 051901
[13] CMS Collaboration 2011 *CMS PAS HIN-11-005* http://cdsweb.cern.ch/record/1361385
[14] ALICE Collaboration 2010 *Phys. Rev. Lett.* **105** 252302
[15] ATLAS Collaboration 2012 *Phys. Lett. B* **707** 330